INVITED PAPER

Crystal structure of 1-propanethiol–Co_2(dobdc) from laboratory X-ray powder diffraction data

Jonathan B. Lefton, Kyle B. Pekar, Daniel Sethio, Elfi Kraka, and Tomče Runčevski [a)]
Department of Chemistry, Southern Methodist University, Dallas, TX 75275, USA

(Received 20 November 2019; accepted 17 January 2020)

Laboratory X-ray powder diffraction was used to solve and refine the crystal structures of appended guest molecules within the pores of metal–organic frameworks (MOFs). Herein, we report the crystal structure of 1-propanethiol adsorbed in the pores of Co_2(dobdc) ($dobdc^{4-}$ = 2,5-dioxido-1,4-benzenedicarboxylate, MOF-74). Soaking the activated MOF in neat 1-propanethiol resulted in the formation of 1-propanethiol–Co_2(dobdc). The thiol appendant MOF maintained the crystal symmetry, with a rhombohedral space group *R*-3 and unit-cell parameters $a = 25.9597(9)$ Å, $c = 6.8623(5)$ Å, and $V = 4005.0(4)$ Å^3. As expected, the thiol sulfur formed a bond with the open cobalt metal site. The alkane chain was directed toward the center of the pore, participating in numerous van der Waals weak interactions with neighboring molecules. For the final Rietveld refinement, soft restrains were applied using bond distances obtained by periodic density functional theory (DFT) geometry optimization. © *2020 International Centre for Diffraction Data.* [doi:10.1017/S0885715620000081]

Key words: MOF, X-ray powder diffraction, crystal structure, Rietveld refinement, geometry optimization

I. INTRODUCTION

Metal–organic frameworks (MOFs) are materials composed of inorganic centers (metal ions or inorganic clusters) and organic linkers self-assembled into a framework structure. The directional covalent bonding between the inorganic and organic counterparts enable ordered crystal structure, with thermal, chemical, and structural stability. With a careful choice of the experimental condition, MOFs maintain their porosity upon removal of the weakly bonded molecules and exhibit permanent porosity with pores of different shape, size, and functionality. One example is the M_2(dobdc) series (M = Mg^{II}, Mn^{II}, Fe^{II}, Co^{II}, Ni^{II}, Cu^{II}, Zn^{II}, and Cd^{II}; $dobdc^{4-}$ = 2,5-dioxido-1,4-benzenedicarboxylate; also referred to as MOF-74 or CPO-27). These MOFs are intensely studied due to their pronounced structural stability and the presence of one-dimensional hexagonal channels decorated by coordinatively unsaturated, open metal(II) sites (Dietzel *et al*., 2006, 2008; Liu *et al*., 2008; Bloch *et al.*, 2011, 2012; Sumida *et al*., 2011; Geier *et al*., 2013; Queen *et al*., 2014; Gonzalez *et al*., 2017).

In order to understand and control the properties of the M_2(dobdc) series of MOFs, it is necessary to elucidate the interactions between the MOF pores and incoming (guest) molecules. In this regard, the interactions of Co_2(dobdc) with various gases (Gonzalez *et al*., 2017) and xylenes isomers (Gonzalez *et al*., 2018) were studied by synchrotron single-crystal X-ray diffraction (SC-XRD). The interactions of Ni_2(dobdc) and Mg_2(dobdc) with noble gases (Magdysyuk *et al*., 2014) were studied by synchrotron X-ray powder diffraction (XRPD). The interactions of various M_2(dobdc) MOFs and CO_2 (Queen *et al*., 2014), H_2 (Sumida *et al*., 2011), hydrocarbons (Bloch *et al.*, 2012), and other molecules were studied by neutron powder diffraction. It is clear that synchrotron X-ray and neutron diffraction studies provide very detailed structural information; however, the availability of these techniques is limited and experiments can be performed only during allocated beamtimes. Laboratory X-ray diffraction methods, on the contrary, are readily available and accessible to various research groups. M_2(dobdc) MOFs do not usually provide high-quality single crystals that are amenable to laboratory SC-XRD studies. That renders XRPD the most suitable technique for routine "in house" studies. To the best of our knowledge, there is no report on a crystal structure of guest–M_2(dobdc) solved and refined from laboratory XRPD data. Herein, we showcase that laboratory XRPD can be used to solve and refine structures of MOFs, and as a case study, we report the crystal structure of 1-propanethiol–Co_2(dobdc). We selected 1-propanethiol due to the presence of a thiol group, which would strongly bind to the open metal site, and a C_3 alkane chain which can freely rotate within the pore.

II. EXPERIMENTAL

A. Sample preparation and data collection

The parent MOF was synthetized following the published procedure (Kizzie *et al*., 2011) with minor modification. 2,5-dihydroxyterephthalic acid (0.964 g, 4.86 mmol) and cobalt nitrate hexahydrate (4.754 g, 16.34 mmol) were added to a 1 l pressure bottle, followed by 400 ml of a 1:1:1 solvent mixture of DMF–ethanol–water. The solvent mixture was sparged with nitrogen gas for 60 min immediately prior to use. Once the solids were dissolved, the bottle was placed in a 100 °C oven for 24 h before removing and cooling to room

[a)]Author to whom correspondence should be addressed. Electronic mail: truncevski@smu.edu

temperature. The mother liquor was decanted off and replaced with 200 ml of DMF, then kept in the oven for 24 h. The DMF soaking process was repeated two additional times, refreshing the DMF once per day. After decanting the DMF for the third time, the same procedure was repeated with methanol three times, with the oven set to 60 °C. Finally, the solid was filtered and dried in air overnight. The Co_2(dobdc) was activated by transferring a small amount to a scintillation vial and heating to 160 °C in an oil bath, under dynamic vacuum, for 18 h. The vial was then transferred to a glovebox for storage waiting for further use. 1-propanethiol–Co_2(dobdc) was prepared by soaking of the MOF in a neat solution of 1-propanethiol for 24 h. The powder was dried under an inert atmosphere and packed in a borosilicate capillary with 0.5 mm diameter. The XRPD pattern (Figure 1) was collected on a laboratory Stoe Stadi-P powder diffractometer, operating in Debye−Scherrer geometry, equipped with a molybdenum X-ray source and monochromatic Mo-$K\alpha$1 radiation obtained by a primary Ge (111) monochromator. The goniometer had two circles (140 and 80 mm). Two linear position-sensitive silicon strip (Mythen Dectris 1K, 50 μm step size) detectors were used to record the scattered X-ray intensity (step size 0.02°, counting time 1 s step^{-1}). Diffraction data were collected at room temperature; additionally, the capillary was rotated for better particle statistics during the measurement.

B. Structure solution and refinement

The XRPD pattern was analyzed with the software TOPAS-Academic V6 (Coelho Software, 2018). Precise unit-cell parameters were obtained by Pawley fitting (Pawley, 1981). The crystal structure was solved by the real-space global optimization simulated annealing (SA) method (Andreev *et al.*, 1997). During the SA runs, the crystal structure of Co_2(dobdc) (Gonzalez *et al.*, 2018) was kept fixed, whereas the position and torsion angles of the 1-propanethiol molecule (defined in *Z*-matrix notation) were freely varied. Once the SA optimization converged to a global minimum, the structure was subjected to Rietveld refinement (Rietveld, 1969). During the refinement, the following parameters were set free: unit cell and peak profile parameters, background

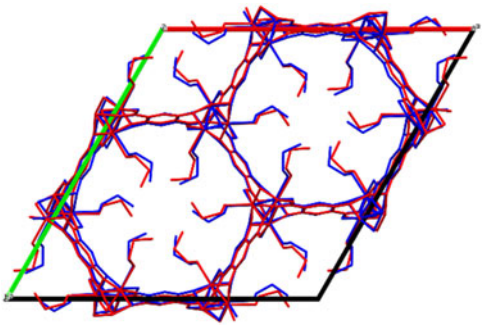

Figure 2. (Color online) An overlap of the crystal packing diagrams of 1-propanethiol–Co_2(dobdc) obtained by SA (blue color) and geometry optimization (red color).

TABLE I. Selected structural, crystallographic and XRPD data collection details.

	1-propanethiol–Co_2(dobdc)
λ (Å)	0.709 30
T (K)	293
2Θ range (°)	1–45
Time (h)	24
Crystal system	Rhombohedral
Space group	*R*-3
a (Å)	25.9597(9)
c (Å)	6.8623(5)
V (Å)	4005.0(4)
R_{exp} (%)[a]	0.0093
R_p (%)[a]	0.0582
R_{wp} (%)[a]	0.0769
R_{Bragg} (%)[a]	0.0248
No. of variables	50

[a]The figures of merit are as defined in TOPAS-Academic V6.

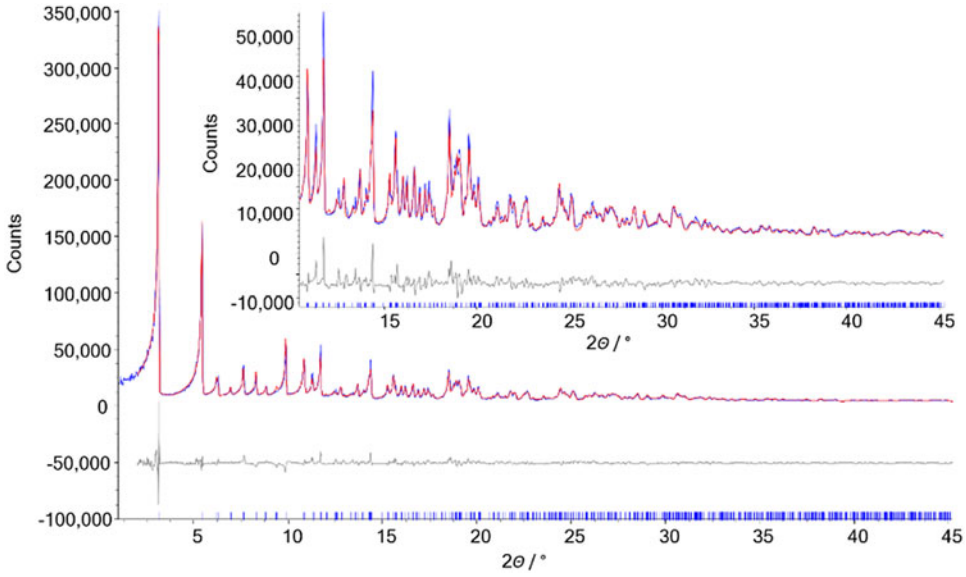

Figure 1. (Color online) Powder diffraction pattern and Rietveld refinement plot for 1-propanethiol–Co_2(dobdc). Measured scattered X-ray intensity is presented as a blue line, the simulated pattern is presented as a red line, the difference curve between the measured and simulated patterns is presented as a gray line, and Bragg reflections are presented as blue bars.

https://doi.org/10.1017/S0885715620000081 Published online by Cambridge University Press

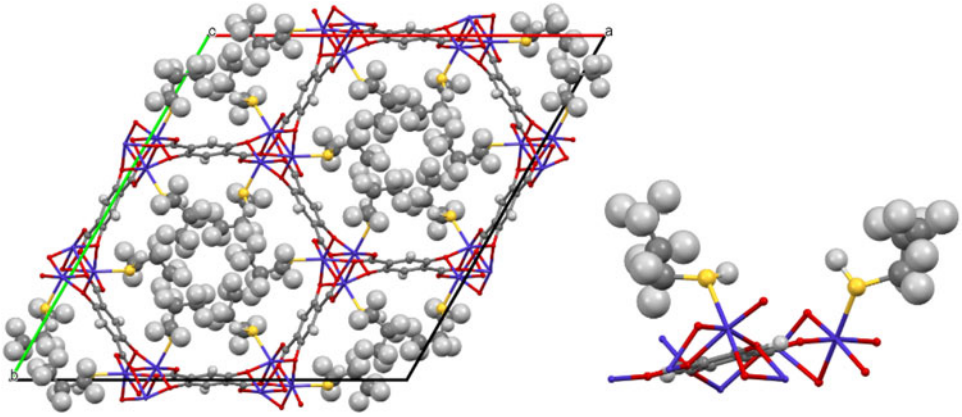

Figure 3. (Color online) Crystal packing diagram of 1-propanethiol–Co_2(dobdc), as obtained by the method of SA. The atoms are presented as ellipsoids, cobalt: blue, oxygen: red, carbon: gray, sulfur: yellow, and hydrogen: white. A fragment of the structure is given in the inset.

coefficients (described as a Chebyshev polynomial), site occupancies, positions of selected atoms (discussed later), and thermal displacement parameters (defined as a single variable for each atomic type, except for hydrogen atoms that were calculated as the thermal displacement parameter of the bonded atom multiplied by a factor of 1.5). The Rietveld plot is given in Figure 2 (and more information is provided in Table 1).

C. Geometry optimization

Geometry optimization including a full relaxation of both atomic positions and lattice parameters was performed using the Crystal17 program package (Dovesi *et al*., 2017). The PBE functional (Perdew *et al*., 1996) augmented with Grimme's D3(BJ) dispersion correction (Grimme *et al*., 2011) was employed in combination with the pob-TZVP basis set (Peintinger *et al*., 2013). The calculation was carried out using the Gilat net (Gilat, 1972) of 8 (65 **k** vectors) in combination with the convergence accuracy of 10^{-7} for the Coulomb and exchange integrals. Vibrational frequency calculation at the center of the Brillouin zone (Γ point) was conducted to ensure the equilibrium geometry corresponds to a minimum on the potential energy surface.

III. RESULTS AND DISCUSSION

The crystal structure solution and refinement of guest molecules adsorbed into porous solids should be performed with particular care, especially when working with (laboratory) powder X-ray diffraction data. There are several factors that could potentially complicate the solution and refinement process. (i) The pores of the MOF may adsorb and host a mixture of different species; for example, molecules of the studied guest compound, mixed with randomly distributed solvent molecules. (ii) Some of the pores may be "clogged" and improperly activated. (iii) The framework structure may exhibit structural dynamics; for example, a rotational disorder of the organic linker. (iv) Guest molecules, such as 1-propanethiol, may exhibit significant rotational disorder especially in the loosely bound, dangling alkane chain.

The crystal structure of 1-propanethiol–Co_2(dobdc) was solved using the global optimization method of SA in direct space. Based on the size of the MOF pores and the kinetic diameter of the guest molecule, the ratio of cobalt and 1-propanethiol was expected to be 1:1. The organic guest molecule was described in *Z*-matrix notation to reduce the degrees of freedom. During the SA runs, an overall atom site occupancy factor was varied along with the position and torsion angles of 1-propanethiol. After the annealing converged to a global minimum, the overall atom site occupancy factor was found to be 0.9, indicating that as much as 10% of the adsorption sites near the open metal sites are either empty or occupied by residual solvent molecules (methanol or dimethylformamide). It should be noted that we performed the same analysis using the diffraction data collected on activated parent MOF. Expectedly, the site occupancy of the 1-propanethiol refined to values close to zero.

Unconstrained Rietveld refinement was challenged by the high degrees of freedom in the structure and by a significant correlation between the refined parameters. This result was expected, considering the complexity of the structure and the limited experimental data. In order to better understand the structural details, the crystal structure of 1-propanethiol–Co_2(dobdc) was optimized using periodic density functional theory, with full relaxation of both atomic positions and lattice parameters. Figure 3 presents an overlap of the crystal packing diagrams obtained by SA and geometry optimization. For the final Rietveld refinement (Figure 1), soft restrains were applied, based on the bond length parameters obtained by the geometry optimization. The crystal structure is presented in Figure 3.

ACKNOWLEDGMENT

We thank the Robert A. Welch Foundation (Grant No.: N-2012-20190330) for financial support.

DEPOSITED DATA

CIF and/or RAW data files were deposited with ICDD. You may request this data from ICDD at info@icdd.com.

Andreev, Y. G., MacGlashan, G. S., and Bruce, P. G. (**1997**). "Ab initio solution of a complex crystal structure from powder-diffraction data using simulated-annealing method and a high degree of molecular flexibility," Phys. Rev. B **55**, 12011–12017.

Bloch, E. D., Murray, L. J., Queen, W. L., Chavan, S., Maximoff, S. N., Bigi, J. P., Krishna, R., Peterson, V. K., Grandjean, F., Long, G. J.,

https://doi.org/10.1017/S0885715620000081 Published online by Cambridge University Press

Smit, B., Bordiga, S., Brown, C. M., and Long, J. R. (**2011**). "Selective binding of O_2 over N_2 in a redox-active metal-organic framework with open iron(II) coordination sites," J. Am. Chem. Soc. **133**, 14814–14822.

Bloch, E. D., Queen, W. L., Krishna, R., Zadrozny, J. M., Brown, C. M., and Long, J. R. (**2012**). "Hydrocarbon separations in a metal-organic framework with open iron(II) coordination sites," Science **335**, 1606–1610.

Dietzel, P. D. C., Panella, P., Hirscher, M., Blom, R., and Fjellvag, H. (**2006**). "Hydrogen adsorption in a nickel based coordination polymer with open metal sites in the cylindrical cavities of the desolvated framework," Chem. Commun. 959–961.

Dietzel, P. D. C., Johnsen, R. E., Fjellvag, H., Bordiga, S., Groppo, E., Chavan, S., and Blom, R. (**2008**). "Adsorption properties and structure of CO_2 adsorbed on open coordination sites of metal–organic framework Ni_2(dhtp) from gas adsorption, IR spectroscopy and X-ray diffraction," Chem. Commun. 5125–5127.

Dovesi, R., Erba, A., Orlando, R., Zicovich-Wilson, C. M., Civalleri, B., Maschio, L., Rèrat, M., Casassa, S., Baima, J., Salustro, S., and Kirtman, B. (**2017**). "Quantum-mechanical condensed matter simulations with CRYSTAL," WIREs Comput. Mol. Sci. **8**, 1360.

Geier, S. J., Mason, J. A., Bloch, E. D., Queen, W. L., Hudson, M. R., Brown, C. M., and Long, J. R. (**2013**). "Selective adsorption of ethylene over ethane and propylene over propane in the metal–organic frameworks M_2(dobdc) (M = Mg, Mn, Fe, Co, Ni, Zn)," Chem. Sci. **4**, 2054–2061.

Gilat, G. (**1972**). "Analysis of methods for calculating spectral properties in solids," J. Comp. Phys. **10**, 432.

Gonzalez, M. I., Mason, J. A., Bloch, E. D., Teat, S. J., Gagnon, K. J., Morrison, G. Y., Queen, W. L., and Long, J. R. (**2017**). "Structural characterization of framework–gas interactions in the metal–organic framework Co_2(dobdc) by in situ single-crystal X-ray diffraction," Chem. Sci. **8**, 4387–4398.

Gonzalez, M. I., Kapelewski, M. T., Bloch, E. D., Milner, P. J., Reed, D. A., Hudson, M. R., Mason, J. A., Barin, G., Brown, C. M., and Long, J. R. (**2018**). "Separation of xylene isomers through multiple metal site interactions in metal−organic frameworks," J. Am. Chem. Soc. **140**, 3412–3422.

Grimme, S., Ehrlich, S., and Goerigk, L. (**2011**). "Effect of the damping function in dispersion corrected density functional theory," J. Comput. Chem. **21**, 1456–1465.

Kizzie, A. C., Wong-Foy, A. G., and Matzger, A. J. (**2011**). "Effect of humidity on the performance of microporous coordination polymers as adsorbents for CO_2 capture," Langmuir **27**, 6368–6373.

Liu, Y., Kabbour, H., Brown, C. M., Neumann, D. A., and Ahn, C. C. (**2008**). "Increasing the density of adsorbed hydrogen with coordinatively unsaturated metal centers in metal−organic frameworks," Langmuir **24**, 4772–4777.

Magdysyuk, O. V., Adams, F., Liermann, H.-P., Spanopoulos, I., Trikalitis, P. N., Hirscher, M., Morris, R. E., Duncan, M. J., McCormick, L. J., and Dinnebier, R. E. (**2014**). "Understanding the adsorption mechanism of noble gases Kr and Xe in CPO-27-Ni, CPO-27-Mg, and ZIF-8," Phys. Chem. Chem. Phys. **16**, 23908–23914.

Pawley, G. S. (**1981**). "Unit-cell refinement from powder diffraction scans," J. Appl. Crystallogr. **14**, 357–361.

Peintinger, M. P., Oliveira, D. V., and Bredow, T. (**2013**). "Consistent Gaussian basis sets of triple-zeta valence with polarization quality for solid-state calculations," J. Comput. Chem. **34**, 451.

Perdew, J. P., Burke, K., and Ernzerhof, M. (**1996**). "Generalized gradient approximation made simple," Phys. Rev. Lett. **77**, 3865–3868.

Queen, W. L., Hudson, M. R., Bloch, E. D., Mason, J. A., Gonzalez, M. I., Lee, J. S., Gygi, D., Howe, J. D., Lee, K., Darwish, T. A., James, M., Peterson, V. K., Teat, S. J., Smit, B., Neaton, J. B., Long, J. R., and Brown, C. M. (**2014**). "Comprehensive study of carbon dioxide adsorption in the metal–organic frameworks M_2(dobdc) (M = Mg, Mn, Fe, Co, Ni, Cu, Zn)," Chem. Sci. **5**, 4569–4581.

Rietveld, H. M. (**1969**). "A profile refinement method for nuclear and magnetic structures," J. Appl. Crystallogr. **2**, 65–71.

Sumida, K., Brown, C. M., Herm, Z. R., Chavan, S., Bordiga, S., and Long, J. R. (**2011**). "Hydrogen storage properties and neutron scattering studiesof Mg_2(dobdc)—a metal–organic framework with open Mg^{2+} adsorption sites," Chem. Commun. **47**, 1157–1159.

https://doi.org/10.1017/S0885715620000081 Published online by Cambridge University Press